LEQG/LTR CONTROLLER DESIGN WITH EXTENDED KALMAN FILTER FOR SENSORLESS INDUCTION MOTOR SERVO DRIVE

Jium-Ming Lin, Hsiu-Ping Wang and Ming-Chang Lin
J Lin: Department of Mechanical Engineering, Chung Hua University, Hsin-Chu.
H Wang & M Lin: Department of Electrical Engineering, Chung Cheng Institute of Technology, Ta-Hsi, Tao-Yuan, Taiwan

Keywords: *linear-exponential-quadratic-gaussian, loop-transfer-recovery, speed sensorless, induction motor servo drives, vector control, extended Kalman filter*

Abstract

In this paper, the Linear Exponential Quadratic Gaussian with Loop Transfer Recovery (LEQG/LTR) methodology is employed for the design of high performance induction motor servo systems. In addition, we design a speed sensorless induction motor vector controlled driver with both the extended Kalman filter and the LEQG/LTR algorithm. The experimental realization of an induction servo system is given. Compared with the traditional PI and LQG/LTR methods, it can be seen that the system output sensitivity for parameter variations and the rising time for larger command input of the proposed method can be significantly reduced.

1 Introduction

Because of the intensive advances of microelectronics and power electronics, the vector controlled induction motor servo drives have become dominant in many applications where fast and precision operations are required[1, 2]. Due to the rapid development in automation technology, the demand for high performance electrical servos has increased. Thus, it is necessary to develop a controller that overcomes the effects of parameter variations, plant uncertainties, and load disturbances.

The Linear Quadratic Gaussian (LQG) method with state feedback technique can provide some guaranteed robustness properties[3]. Also, the adoption of Loop Transfer Recovery (LTR) process can enhance the robustness of system with state observer[4, 5]. Thus, it was extensively applied in the design of motor drive systems[6, 7, 8, 9]. On the other hand, some papers[10, 11, 12, 13] concluded that the optimal control systems obtained by the Linear Exponential Quadratic Gaussian and Loop Transfer Recovery (LEQG/LTR) methods were insensitive to the load disturbances and sensor noises. This is due to that the LEQG/LTR method can take the covariances of both system and measurement noises into consideration. So far, the LEQG/LTR technique has not been applied to the design of induction motors yet, this paper is the first one.

We can see that applying the proposed method to the design of an induction motor servos with speed sensor, the loop transfer functions can be shaped, so that the closed-loop systems will yield better performances than those obtained by the PI and LQG/LTR methods[9] in command following, output disturbance rejection, and robustness to noises and unmodeled system dynamics. Aside, a speed sensorless vector controlled induction motor drive[14, 15] by using the extended Kalman filter[16] and the LEQG/LTR algorithm is derived. The experimental results illustrate that the system output sensitivity for load and command amplitude, and the rising time for larger command can be reduced while comparing to the PI and LQG/LTR controllers.

The rests of this paper are organized as follow. In Section 2, the proposed method is formulated and applied for an induction motor servo drive system design. In Section 3, the experiment results are given to demonstrate the effectiveness of the proposed method. Finally, brief conclusions are drawn in Section 4.

2 Problem and Methodology Formulation

2.1 Induction Motor Formulation

Consider an induction motor servo, the state equation in the rotating reference frame is[8, 9]

$$\begin{bmatrix} \dot{i}_{\gamma s} \\ \dot{i}_{\delta s} \\ \dot{\phi}_{\gamma r} \\ \dot{\phi}_{\delta r} \end{bmatrix} = \begin{bmatrix} \Xi & \omega \\ -\omega & \Xi \\ \frac{MR_r}{L_r} & 0 \\ 0 & \frac{MR_r}{L_r} \end{bmatrix}$$

$$
\begin{bmatrix} \frac{MR_r}{\sigma L_s L_r^2} & \frac{\omega_{re}M}{\sigma L_s L_r} \\ -\frac{\omega_{re}M}{\sigma L_s L_r} & \frac{MR_r}{\sigma L_s L_r^2} \\ -\frac{R_r}{L_r} & \omega-\omega_{re} \\ -\omega+\omega_{re} & -\frac{R_r}{L_r} \end{bmatrix} \begin{bmatrix} i_{\gamma s} \\ i_{\delta s} \\ \phi_{\gamma r} \\ \phi_{\delta r} \end{bmatrix}
+\frac{1}{\sigma L_s}\begin{bmatrix} v_{\gamma s} \\ v_{\delta s} \\ 0 \\ 0 \end{bmatrix}, \tag{1}
$$

where $\Xi = -\frac{R_s}{\sigma L_s} - \frac{R_r(1-\sigma)}{\sigma L_r}$, $(i_{\gamma s}, i_{\delta s})$ are the stator currents, $(\phi_{\gamma r}, \phi_{\delta r})$ are the rotor fluxes, $(v_{\gamma s}, v_{\delta s})$ are the stator voltages respectively in the γ- and δ-axis, ω is the operating angular frequency of AC, ω_{re} is the electrical angular velocity of rotor, $\sigma = 1 - \frac{M^2}{L_s L_r}$ is total leakage factor, and R_s, R_r, L_s, L_r, and M are the stator, rotor resistances, stator, rotor, and mutual inductances.

If one let

$$
\omega - \omega_{re} \overset{\triangle}{=} \omega_{se} = \frac{MR_r i_{\delta s}}{L_r \phi_{\gamma r}}, \tag{2}
$$

where ω_{se} is the slip rate, and let $\phi_{\delta r} = 0$, then we have, from the last row of Eq.(1),

$$
\begin{aligned}
T_e &= p\frac{M}{L_r}\phi_{\gamma r} i_{\delta s}, && (3)\\
\dot{\phi}_{\gamma r} &= -\frac{R_r}{L_r}\phi_{\gamma r} + \frac{MR_r}{L_r} i_{\gamma s}, && (4)
\end{aligned}
$$

where p is the number of poles.

By Eqs.(3) and (4), Eq.(1) can be rewritten as

$$
\begin{bmatrix} i_{\gamma s} \\ i_{\delta s} \\ \phi_{\gamma r} \end{bmatrix} = \begin{bmatrix} \Xi & 0 & \frac{MR_r}{\sigma L_s L_r^2} \\ 0 & -\frac{R_s}{\sigma L_s} & 0 \\ \frac{MR_r}{L_r} & 0 & -\frac{R_r}{L_r} \end{bmatrix} \begin{bmatrix} i_{\gamma s} \\ i_{\delta s} \\ \phi_{\gamma r} \end{bmatrix} + \begin{bmatrix} \frac{v'_{\gamma s}}{\sigma L_s} \\ \frac{v'_{\delta s}}{\sigma L_s} \\ 0 \end{bmatrix} \tag{5}
$$

where

$$
\begin{aligned}
v_{\gamma s} &= v'_{\gamma s} - \omega\sigma L_s i_{\delta s}, && (6)\\
v_{\delta s} &= v'_{\delta s} + \omega(\sigma L_s i_{\delta s} + \frac{M}{L_r}\phi_{\gamma r}), && (7)
\end{aligned}
$$

and $v'_{\gamma s}$, $v'_{\delta s}$ mean the current controller outputs of $i_{\gamma s}$ and $i_{\delta s}$, respectively.

if one let $\dot{\phi}_{\gamma r} = 0$, then $i^\star_{\delta s} = i_{\delta s}$ and the torque can be controlled by the δ-axis stator current $i^\star_{\delta s}$, then we have, by Eq.(5),

$$
\begin{aligned}
\phi_{\gamma r} &= M i_{\gamma s}, && (8)\\
(\sigma L_s + R_s) i^\star_{\delta s} &= v'_{\delta s}, && (9)
\end{aligned}
$$

where $i^\star_{\delta s}$ is the command input of torque current.

By Eqs.(2) and (5), we have

$$
\begin{aligned}
\omega_{se} &= \frac{R_r}{L_r i_{\gamma r}} i^\star_{\delta s}, && (10)\\
v'_{\delta s} &= v_{\delta s} - \omega_{re}\Lambda i_{\gamma s} - \frac{R_r}{L_r}\Lambda i^\star_{\delta s}, && (11)
\end{aligned}
$$

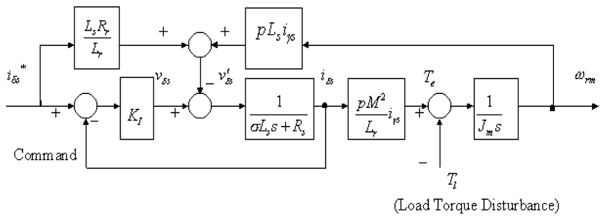

Fig. 1 Block diagram of a decoupling current-controlled induction servo drive system

where $\Lambda = (\sigma L_s + \frac{M^2}{L_r})$, we hence have

$$
v'_{\delta s} = v_{\delta s} - p\omega_{rm} L_s i_{\gamma s} - \frac{R_r L_s}{L_r} i^\star_{\delta s}, \tag{12}
$$

where ω_{rm} is the mechanical angular velocity of rotor. If the effects of windage viscousity and bearing friction are negligible, the block diagram of the decoupling current-controlled servo drive is shown in Figure 1, where K_I is the equivalent current loop gain.

Define

$$
\frac{L_s R_r}{L_r} = K_F\,,\ pL_s i_{\gamma s} = K_E\,,\ \frac{pM^2}{L_r} i_{\gamma s} = K_T\,. \tag{13}
$$

Then the equivalent model of the vector controlled induction motor drive can be approximated as[9]

$$
\begin{aligned}
G_p(s) &= \frac{(K_I - K_F)K_T}{(\sigma L_s J_m)s^2 + (R_s + K_I)J_m s + K_E K_T}\\
&= \frac{K'}{(s\tau_e + 1)(s\tau_m + 1)}, && (14)
\end{aligned}
$$

where K_I is the equivalent dc gain, and τ_e, τ_m are the equivalent electrical and mechanical time constants, respectively.

2.2 Standard LEQG/LTR Design

Consider a Linear Time-Invariant (LTI), controllable and observable stochastic system

$$
\begin{aligned}
\dot{x}(t) &= Ax(t) + Bu(t) + \Gamma w(t),\\
y(t) &= Cx(t) + v(t), && (15)
\end{aligned}
$$

where $x(t)$, $u(t)$, and $y(t)$ are the state, control, and measurement vectors, and $w(t)$ and $v(t)$ are the uncorrelated Gaussian white noises with zero-mean and covariances

$$
\begin{aligned}
E\{w(t)w^T(\tau)\} &= W\delta(t-\tau),\ W > 0 && (16)\\
E\{v(t)v^T(\tau)\} &= V\delta(t-\tau),\ V > 0 && (17)\\
E\{v(t)w^T(\tau)\} &= 0, && (18)
\end{aligned}
$$

respectively, where $E\{\bullet\}$ is an expectation function operator. The problem is then to derive a feedback-control law which minimizes the following quadratic cost function:

$$J = \alpha E\left\{ e^{\left[\alpha \int_0^T (Z^T(t)QZ(t)+u^T(t)Ru(t)dt)\right]} \right\}, \tag{19}$$

where $e^{[\bullet]}$ is an exponential function operator, $Z = Nx$ is a linear combination of the states, Q is a semi-positive definite weighting matrix, R is a positive definite weighting matrix, and α is a dimensionless weighting factor.

The solution to the LEQG problem is described by the separation principle, which states that the optimal result is achieved by two steps[4, 5]. First, obtain an optimal estimate $\hat{x}$ of the state x, and then use this estimated state as if it were an exact measurement of the state, to solve the Linear Exponential Quadratic Regulator (LEQR) problem. Namely, the solution to the first step is given by Kalman-filter theory. The second step is to find the optimal control input of a LEQR problem to minimize the performance cost. The block diagram of the system with the LEQG-based controller is referred to Figure 2. The robustness

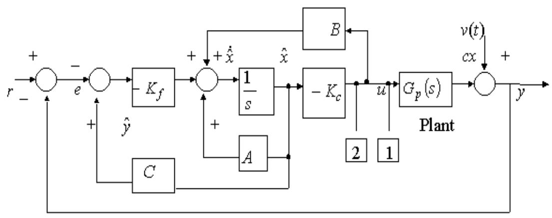

Fig. 2 The block diagram of the system with the LEQG-based compensator

and performance properties at the input of the plant are determined by the return ratio at the point marked 1 in Figure 2, whereas the return ratio $(-K_c(sI-A)^{-1}B)$, which is the one we would like to have, is the return ratio at the point marked 2. It is often desired to design the return ratio at the output of the plant rather than the input. In this case we can follow the procedures,

S1: Design a Kalman filter by manipulating the covariance matrices W and V until a return ratio $-C(sI-A)^{-1}K_f$ is obtained which would be satisfactory at the plant output.

S2: Synthesize an optimal state-feedback regulator by setting $M = C$, $Q = Q_0 + qI$ and $R = I$ (or $Q = I$ and $R = \rho I$), and increase q (or reduce ρ) until the return ratio at the output of the compensated plant has converged sufficiently closely to $-C(j\omega I - A)^{-1}K_f$ over a sufficiently large range of frequencies.

The standard form of the LEQG-based controller is given by

$$\begin{aligned} \dot{\hat{x}}(t) &= A_c\hat{x}(t) + K_f e(t), & (20)\\ u(t) &= -K_c\hat{x}(t), & (21) \end{aligned}$$

where

$$\begin{aligned} A_c &= A - BK_c - K_fC, & (22)\\ K_f &= P_fCV^{-1}, & (23)\\ K_c &= R^{-1}B^TP_c, & (24) \end{aligned}$$

by P_f and P_c satisfied with the algebraic Riccati equations,

$$\begin{aligned} 0 &= P_fA^T + AP_f + \Gamma W \Gamma^T \\ &\quad -P_fC^TV^{-1}CP_f, & (25)\\ 0 &= P_cA + A^TP_c + Q \\ &\quad -P_c(BR^{-1}B^T - \alpha K_fVK_f^T)P_c. & (26) \end{aligned}$$

2.3 Speed Estimation Method

Let the discrete induction motor system be

$$\begin{aligned} X(k+1) &= A_d(k)X(k) + B_d(k)U(k) \\ &\quad +w(k) & (27)\\ Z(k) &= H(k)X(k) + v(k), & (28) \end{aligned}$$

where

$$\begin{aligned} X(k) &= \left[i_{\gamma s}(k)\ i_{\delta s}(k)\ \phi_{\gamma r}(k)\ \phi_{\delta r}(k)\right]^T, & (29)\\ U(k) &= \left[v_{\gamma s}(k)\ v_{\delta s}(k)\right]^T, & (30)\\ A_d(k) &= e^{A(k)T_s} \cong I + A(k)T_s, & (31)\\ B_d(k) &= \int_0^{T_s} e^{A(k)\tau}B(k)d\tau \cong B(k)T_s, & (32)\\ H(k) &= \begin{bmatrix} 1 & 0 & 0 & 0 \\ 0 & 1 & 0 & 0 \end{bmatrix}, & (33) \end{aligned}$$

where T_s is the sampling period.
The nonlinear motor drive can be modified as[15]

$$\begin{aligned} X(k+1) &= f(X(k),U(k)) + w(k) & (34)\\ Z(k) &= h(X(k)) + v(k), & (35) \end{aligned}$$

where

$$\begin{aligned} X(k) &= \left[\omega_{re}(k)\ R_r(k)\ i_{\gamma s}(k)\right. \\ &\quad \left. i_{\delta s}(k)\ \phi_{\gamma r}(k)\ \phi_{\delta r}(k)\right], & (36)\\ U(k) &= \left[v_{\gamma s}(k)\ v_{\delta s}(k)\right]^T, & (37)\\ x_1(k+1) &= x_1(k) + w_1(k), & (38)\\ x_2(k+1) &= x_2(k) + w_2(k), & (39)\\ x_3(k+1) &= \chi x_3(k) + T_s\omega x_4(k) \\ &\quad +\zeta x_2(k)x_5(k) + \eta x_1(k)x_6(k) \\ &\quad +\frac{T_s}{\sigma L_s}v_1(k) + w_3(k), & (40)\\ x_4(k+1) &= -T_s\omega x_3(k) + \chi x_4(k) \\ &\quad -\eta x_1(k)x_5(k) + \zeta x_2(k)x_6(k) \\ &\quad +\frac{T_s}{\sigma L_s}v_2(k) + w_4(k), & (41)\\ x_5(k+1) &= \kappa x_3(k) + \nu x_5(k) \end{aligned}$$

$$
\begin{aligned}
& && +\varepsilon x_6(k)+w_5(k), && (42)\\
x_6(k+1) &=& & \kappa x_4(k)-T_s\varepsilon x_5(k) && \\
& && +\nu x_6(k)+w_6(k), && (43)\\
z_1(k) &=& & i_{\gamma s}(k)+v_1(k), && (44)\\
z_2(k) &=& & i_{\delta s}(k)+v_2(k), && (45)\\
w(k) &=& & [w_1(k)\ w_2(k)\ w_3(k) && \\
& && w_4(k)\ w_5(k)\ w_6(k)], && (46)\\
v(k) &=& & [v_1(k)\ v_2(k)]^T, && (47)
\end{aligned}
$$

where $\chi = 1 - T_s\left[\frac{R_s}{\sigma L_s} + \frac{(1-\sigma)x_2(k)}{\sigma L_r}\right]$, $\eta = \frac{T_s M}{\sigma L_s L_r^2}$, $\zeta = \frac{T_s M}{L_r}$, $\kappa = \frac{T_s M x_2(k)}{L_r}$, $\varepsilon = T_s(\omega - x_1(k))$, *and* $\nu = \left[1 - \frac{T_s x_2(k)}{L_r}\right]$.

The linearized system of Eqs.(34) and (35) can be written as

$$
\begin{aligned}
X(k+1) &= F(k)X(k)+w(k) && (48)\\
Z(k) &= \Delta(k)X(k)+v(k), && (49)
\end{aligned}
$$

where

$$
F(k) = \frac{\partial f(X(k),U(k))}{\partial X(k)}\Big|_{X(k)=\hat{X}(k|k)} \quad (50)
$$

$$
= \begin{bmatrix}
1 & 0 & 0 & 0 & 0 & 0\\
0 & 1 & 0 & 0 & 0 & 0\\
\zeta x_6(k) & T_s\vartheta & \chi & T_s\omega & \eta x_2(k) & \zeta x_1(k)\\
-\zeta x_5(k) & T_s\iota & -T_s\omega & \chi & -\zeta x_1(k) & \eta x_2(k)\\
-T_s x_6(k) & \xi & \kappa & 0 & \nu & \varepsilon\\
T_s x_5(k) & \varsigma & 0 & \kappa & -\varepsilon & \nu
\end{bmatrix}, \quad (51)
$$

$$
\Delta(k) = \frac{\partial h(X(k))}{\partial X(k)}\Big|_{X(k)=\hat{X}(k|k)}
$$

$$
= \begin{bmatrix} 0 & 0 & 1 & 0 & 0 & 0\\ 0 & 0 & 0 & 1 & 0 & 0 \end{bmatrix}, \quad (52)
$$

where $\vartheta = \rho x_3(k) + \eta x_5(k)$, $\iota = \rho x_4(k) + \eta x_6(k)$, $\xi = T_s\left[\frac{M x_3(k)}{L_r} - \frac{x_5(k)}{L_r}\right]$, $\rho = \frac{(1-\sigma)}{\sigma L_r}$ and $\varsigma = T_s\left[\frac{M x_4(k)}{L_r} - \frac{x_6(k)}{L_r}\right]$.

Next, we use the flowing Kalman filter to estimate speed,

$$
\begin{aligned}
\hat{X}(k\mid k-1) &= f\left(\hat{X}(k-1\mid k-1),U(k-1)\right) && (53)\\
P(k\mid k-1) &= F(k)P(k-1\mid k-1)F^T(k) && \\
&\quad +Q(k-1), && (54)\\
K(k) &= P(k\mid k-1)\Delta^T[\Delta(k)P(k\mid k-1) && \\
&\quad \Delta^T(k)+R(k)]^{-1}, && (55)\\
\hat{X}(k\mid k) &= \hat{X}(k\mid k-1)+K(k)[Z(k) && \\
&\quad -H(k)\hat{X}(k\mid k-1)], && (56)\\
P(k\mid k) &= [I-K(k)H(k)]P(k\mid k-1), && (57)
\end{aligned}
$$

where K is the Kalman-filter gain, $\hat{X}$ is the estimated state, and Q is a 6×6 constant matrix.

3 Experimental Results

This model is taken from the catalog of TECO 3-phase induction motor (TYPE : AEEF) with four poles, the parameters are shown in Table 1. The load applies OGURA PB-1.2 brake, and the tachometer series number is MICROTECH MES-30-1000-E-K5.

Table 1: Parameters list

Stator resistance	$R_s = 3.2931\Omega$
Rotor resistance	$R_r = 2\Omega$
Stator inductance	$L_s = 0.1462H$
Rotor inductance	$L_r = 0.1439H$
Mutual inductance	$M = 0.1391H$
Lumped inertia	$J = 0.009NMS^2$
Number of poles	$p = 4$

From Eqs.(13), we can find

$$
K_F = 2.03, K_E = 0.29 i_{\gamma s}, K_T = 0.27 i_{\gamma s}, \quad (58)
$$

Let $i_{\gamma s} = 3.5A$, then $K_E = 1.02$, and $K_T = 0.94$. If we choose $K_I = 100$, then the transfer function of Eq.(14) becomes

$$
G_p(s) = \frac{922095}{s^2+9296s+9632}, \quad (59)
$$

S1: *Kalman-filter Gain Design*

For the target feedback loop design, we need to set the matrices Γ, W and V in advance, then solve Eq.(25) to find P_f, and finally obtain the Kalman-filter gain K_f from Eq.(23). This procedure is similar to solve the Equation of a Linear Quadratic problem, thus in the following, we shall abbreviate the formulation of this step as

$$
K_f = LQE(A,\Gamma,C,W,V). \quad (60)
$$

Generally, it is advisable to start with simple choices of Γ, W, and V, then inspect the resulting Kalman-filter return ratio. One set of possible choice is $\Gamma = B$ [3], $W = 1$, $V = \mu$. Thus, we have

$$
K_f = LQE(A,B,C,1,\mu). \quad (61)
$$

After some trial-and-error, we choose $\mu = 1$, then

$$
K_{f1} = \begin{bmatrix} 0.0055\\ 0.0001 \end{bmatrix}. \quad (62)
$$

For the sake to make the steady-state error be zero, the first thing is to insert integral action to each input. As it was mentioned [**?**], placing poles of the augmented model at the origin would lead to problems in the recovery step later, so in this case we place them at -0.0001. Then the system model of this integrator can be expressed as

$$
A_w = -10^{-4},\ B_w = 1,\ C_w = 1,\ D_w = 0. \quad (63)
$$

The augmented system model is[12]

$$A_a = \begin{bmatrix} A & \Gamma C_w \\ 0 & A_w \end{bmatrix}, \quad B_a = \begin{bmatrix} B \\ 0 \end{bmatrix},$$
$$\Gamma_a = \begin{bmatrix} \Gamma D_w \\ B_w \end{bmatrix}, \quad C_a = [C \; 0]. \tag{64}$$

Now we have the new Kalman gain matrix as

$$K'_{f1} = LQE(A_a, \Gamma_a, C_a, 1, 1) = \begin{bmatrix} 10^{-4} \\ 0 \\ 1 \end{bmatrix}. \tag{65}$$

Define the sensitivity function

$$S_F(s) = \left[I + C_a(sI - A_a)^{-1} K'_{f1}\right], \tag{66}$$

and the closed-loop transfer function is

$$T_F(s) = I - S_F(s). \tag{67}$$

The principal gain of the return ratio $-C(sI - A)^{-1}K'_{f1}$ is shown in Figure 3, Figure 4 shows the principal gains of the sensitivity function $S_F(s)$ and the closed-loop transfer function $T_F(s)$. From $T_F(s)$ it can be seen that the steady-state error of the system is reduced to zero by inserting integral action to each input.

S2: *LEQG/LTR Compensator Gain Design*
Let $N = C_a$, $Q = I$, $R = \rho I$ and $W = I$, then we have the Hamiltonian matrix of the LEQG problem defined as

$$\begin{bmatrix} \dot{X} \\ \dot{P} \end{bmatrix} = \begin{bmatrix} A_a & -\frac{1}{2}B_a\rho^{-1}B_a^T + \frac{1}{2}\Gamma_a \alpha W \Gamma_a^T \\ -2C_a^T C_a & -A_a^T \end{bmatrix} \begin{bmatrix} X \\ P \end{bmatrix}, \tag{68}$$

where X is the state vector, and P is the Lagrange multiplier. Thus by Eqs.(64), (24) and (26), one can obtain the optimal control gain K_c. Choose $\alpha = 100$ and $\rho = 1$, then by Eq. (24) we have

$$K_{c1} = \begin{bmatrix} 7 & 70345 & -1 \end{bmatrix}. \tag{69}$$

Once the control gain K_c has been found, a state-space realization of the compensator $K(s)$ is given by $(A_{K1}, B_{K1}, C_{K1}, D_{K1})$, where

$$A_{K1} = A_a - B_a K_{c1} - K'_{f1} C_a, \tag{70}$$
$$B_{K1} = K'_{f1}, \tag{71}$$
$$C_{K1} = -K_{c1}, \tag{72}$$
$$D_{K1} = 0. \tag{73}$$

Thus the sensitivity and co-sensitivity functions are

$$S(s) = [I + C_{K1}(sI - A_{K1})^{-1}B_{K1}] \tag{74}$$
$$T(s) = I - S(s). \tag{75}$$

Figure 5 shows the principal gain of $K(s)G_p(s)$, the principal gains of the sensitivity function $S(s)$ and the closed-loop transfer function $T(s)$ are shown in Figure 6. The closed-loop step and impulse responses are shown in Figures 7 and 8, respectively.

S3: *Digitize LEQG/LTR Controller*
Let the sampling period be 100 μsec, then we have the system matrices of digital controller

$$A_{DK1} = \begin{bmatrix} 0.388 & -5.52 & 10^{-4} \\ 10^{-4} & 0.99 & 0 \\ -0.003 & -87.2 & 1 \end{bmatrix} \tag{76}$$
$$B_{DK1} = \begin{bmatrix} 10^{-4} \\ 0 \\ 0.999 \end{bmatrix}, \tag{77}$$
$$C_{DK1} = \begin{bmatrix} -8 \cdot 10^{-4} & -7.029\ 10^{-4} \end{bmatrix}, \tag{78}$$
$$D_{DK1} = -3 \cdot 10^{-5}. \tag{79}$$

S4: *Experimental Realization*

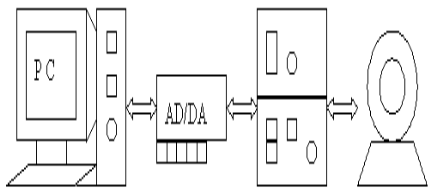

Fig. 9 System configuration of the experiment

(a) *With speed sensor*
The system configuration of the experiment is shown in Figure 9.

i. PI-based design[1].
The results of no load for the square-wave rotation speed input ω^*_{rm} with amplitudes 600 and 1800 rad/s are shown in Figure 10. The responses with 1 N load are shown in Figure 11. It can be seen that there is chattering effect for the case of $\omega^*_{rm} = 600\ rad/s$, and the rising time of the response is larger with $\omega^*_{rm} = 1800\ rad/s$.

ii. LQG/LTR-based design
The responses by using LQG/LTR method with the same design parameters are shown in Figures 12 and 13. It can be seen that there is overshoot for the no load case with$\omega^*_{rm} = 600\ rad/s$.

[1]The PI coefficients, $K_P = 6$ and $K_I = 2400$, are designed for the same bandwidth as LEQG/LTR method.

iii. LEQG/LTR-based design
The responses by using LEQG/LTR method are shown in Figures 14 and 15. It can be seen that the results obtained by the proposed method are better for comparing with the other methods aforementioned.

(b) *Sensorless*
The speed sensor is replaced by the extended Kalman-filter.

i. PI-based design
The results are shown in Figures 16 and 17. From the responses, we can find that there are vibratory effects in low speed, and the rise times are larger for the high speed command responses with and without load.

ii. LQG/LTR-based design
The responses by using LQG/LTR method are shown in Figures 18 and 19. It can be seen that for the case with $\omega_{rm}^{\star} = 600\ rad/s$ there is vibratory in low speed. Also, the rising times with $\omega_{rm}^{\star} = 1800\ rad/s$ are also large for the response with and without load.

iii. LEQG/LTR-based design
The results for LEQG/LTR-based controller are shown in Figures 20 and 21. The results are still better despite of some small or shake effects.

4 Conclusions

In this paper, the LEQG/LTR method is applied for the servo controller design. A systematic design procedure is proposed. In addition, we design a speed sensorless induction motor vector controlled driver with both the extended Kalman-filter and the LEQG/LTR algorithm. Performance comparisons with load disturbance and parameter variations by experimental realization are also carried out. It can be seen that by using the proposed method to the design of induction motor servo drive system, the loop transfer functions can be shaped so that the closed-loop systems will yield (1) good command following, and (2) good output disturbance rejection, which are better than those obtained by the well-known PI and LQG/LTR methods.

Acknowledgment

This work was supported by the National Science Council of the R.O.C. under grant no. NSC-89-2218-E-216-001.

References

[1] R. Gabriel, W. Leonhard, and C. J. Nordby, "Field-oriented control of a standard AC motor using microprocessors", *IEEE Transaction on Industrial Application*, vol. 16, Mar./Apr. 1980, pp. 186-192.

[2] F. Harashima, S. Kondo, K. Ohnishi, M. Kajita, and M. Susono, "Multimicroprocessor-based control system for quick response induction motor drive", *IEEE Transaction on Industrial Application*, vol. 21, May/June 1985, pp. 602-609.

[3] J. M. Maciejowski, "Multivariable feedback design", *addison-wesley publishing company*, 1989.

[4] J. C. Doyle and G. Stein, "Multivariable feedback design: concepts for a classical/modern synthesis",*IEEE Transactions on Automatic Control*, vol. AC-26, No. 1, 1981, pp. 4-16.

[5] G. Stein and M. Athans, "The LQG/LTR procedure for multivariable feedback control design ", *IEEE Transactions on Automatic Control*, vol. 32, Feb, 1987, pp. 105-106.

[6] J. K. Ji and S. K. Sul,"LQG based speed controller for torsional vibration suppression in 2-mass system", in *IEEE IECON'93*, 1993, pp. 1157-1162.

[7] J. K. Ji and S. K. Sul, "Kalman filter and LQ based speed controller for torsional vibration suppression in a 2-mass motor drive system", *IEEE Transactions on Industrial Electronics*, vol. 42, No. 6, December, 1995, pp. 564-571.

[8] H. Hanselmann and A. Engelke, "LQG-Control of a highly resonant disk drive head positioning actuator", *IEEE Transactions on Industrial Electron*, vol. 35, Fed. 1988, pp. 100-104.

[9] Y. Y. Tzou and H. J. Wu, "LQG/LTR control of an AC induction servo drive", *IEEE Transactions on Power Electronics*, vol. 10. No. 2, March 1995, pp. 214-221.

[10] D. H. Jacobson, "Optimal stochastic linear systems with exponential performance criteria and their relation to deterministic differential games", *IEEE Transactions on Automatic Control*, Vol. AC-18, No.2, 1973, pp. 124-131.

[11] J. L. Speyer, J. J. Deyst, and D. H. Jacobson, "Optimization of stochastic linear systems

with additive measurement and process noise using exponential performance criteria", *IEEE Transactions on Automatic Control*, Vol. AC-19, No.10, 1974, pp. 358-366.

[12] J. L. Speyer, "An adaptive terminal guidance scheme basedom an exponential cost criteria", *IEEE Transactions on Automatic Control*, June 1976, pp. 660-665.

[13] J. M. Lin, "Bank-to-Turn optimal guidance with linear exponential gaussian performance index and constant acceleration bias", *Proc. of Amer. Control*, Conference, Boston, June 1991, pp. 26-28.

[14] Y. R. Kim, S. K. Sul, and M. H. Park, "Speed sensorless vector control of induction motor using extended Kalman filter", *IEEE Transactions on Application*, Vol. 30, No.5, September/October 1994, pp. 1225-1233.

[15] Y. S. Kim, S. U. Kim, and I. W. Yang, "Implementation of a speed sensorless vector control of induction motor by reduced-order extended Kalman filter", *IEEE Transactions on Power Electronics*, *Conference and Exposition*, Vol. 1, 1994, pp. 1225-1233.

[16] J. M. Mendel, "Lessons in estimation the theory for signal processing, communications, and control", *Prentice-Hall International*, Inc., 1995.

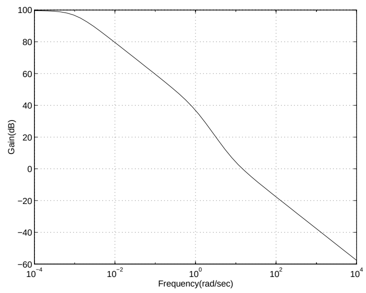

Fig. 3 Priciple gain of $-C(sI-A)^{-1}K'_{f1}$.

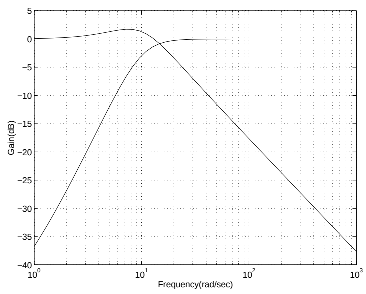

Fig. 4 Priciple gain of $S_F(s)$ and $T_F(s)$.

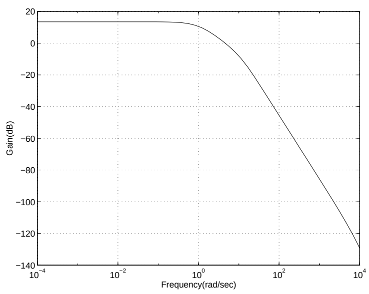

Fig. 5 Principle gain of $K(s)G_p(s)$.

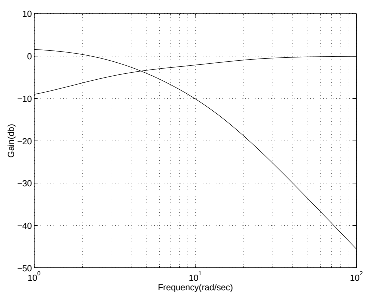

Fig. 6 Principle gain of $S(s)$ and $T(s)$.

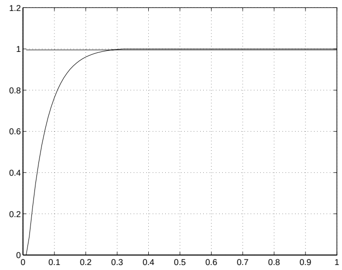

Fig. 7 Closed-loop unit step input response.

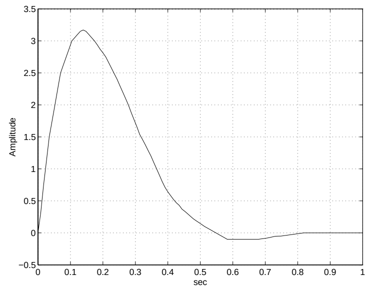

Fig. 8 Closed-loop impulse response.

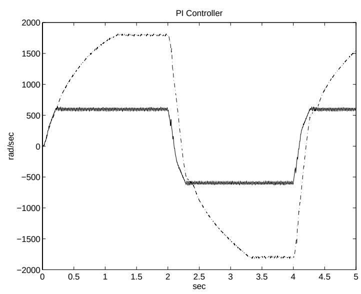

Fig. 10 The speed response w/o load and w/ $\omega^{\star}_{rm} =$ 600 and 1800 rad/s (dashed line).

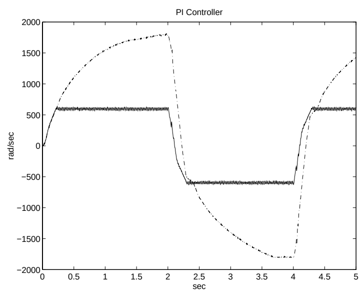

Fig. 11 The speed response w/ 1 N load and w/ $\omega^{\star}_{rm} =$ 600 and 1800 rad/s (dashed line).

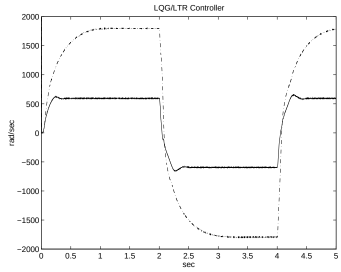

Fig. 12 The speed response w/o load and w/ $\omega^{\star}_{rm} =$ 600 and 1800 rad/s (dashed line).

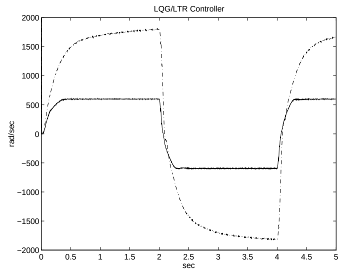

Fig. 13 The speed response w/ 1 N load and w/ $\omega^{\star}_{rm} =$ 600 and 1800 rad/s (dashed line).

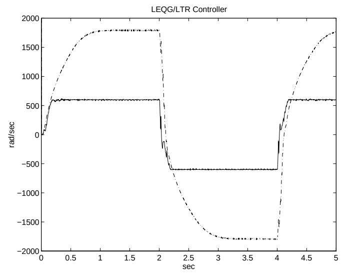

Fig. 14 The speed response w/o load and w/ $\omega^{\star}_{rm} =$ 600 and 1800 rad/s (dashed line).

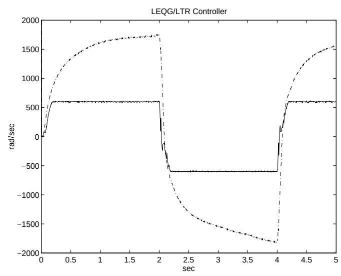

Fig. 15 The speed response w/o load and w/ $\omega^{\star}_{rm} =$ 600 and 1800 rad/s (dashed line).

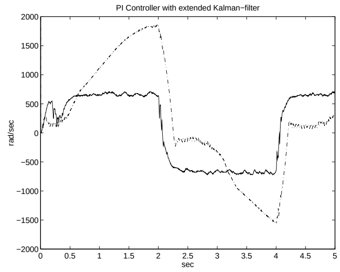

Fig. 16 The speed response w/o load and w/ $\omega^{\star}_{rm} =$ 600 and 1800 rad/s (dashed line).

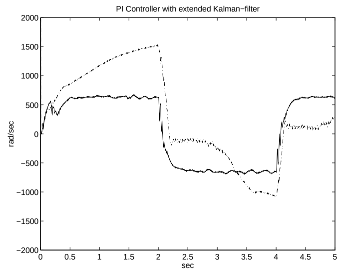

Fig. 17 The speed response w/ 1 N load and w/ $\omega^{\star}_{rm} =$ 600 and 1800 rad/s (dashed line).

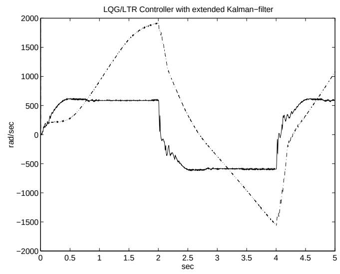

Fig. 18 The speed response w/o load and w/ $\omega^{\star}_{rm} =$ 600 and 1800 rad/s (dashed line).

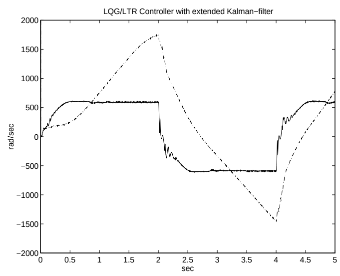

Fig. 19 The speed response w/ 1 N load and w/ $\omega^{\star}_{rm} =$ 600 and 1800 rad/s (dashed line).

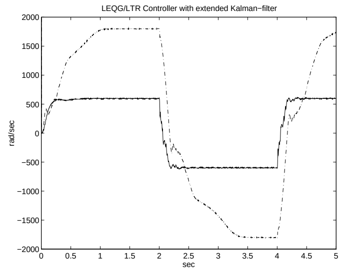

Fig. 20 The speed response w/o load and w/ $\omega^{\star}_{rm} =$ 600 and 1800 rad/s (dashed line).

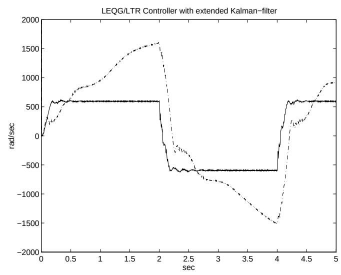

Fig. 21 The speed response w/ 1 N load and w/ $\omega^{\star}_{rm} =$ 600 and 1800 rad/s (dashed line).